17th International Conference on Environmental Science and Technology

Athens, Greece, 1 to 4 September 2021

Preparation and Characterization of f-MWCNT-GO Self-assembled Polymeric Nanocomposite Membrane for Wastewater Treatment

NASSAR L.[1,*], KHALIL H.[1], WADI V.[2], NADDEO V.[3], BANAT F.[4] and HASAN S.[4]

[1]Center for Membranes and Advanced Water Technology (CMAT), Water and Environmental Engineering, Khalifa University of Science and Technology, Abu Dhabi, UAE

[2]Department of Chemistry, Khalifa University of Science and Technology, Abu Dhabi, UAE

[3]Sanitary Environmental Engineering Division (SEED), Department of Civil Engineering, University of Salerno, Fisciano (SA), Italy

[4]Department of Chemical Engineering, Khalifa University of Science and Technology, Abu Dhabi, UAE

*corresponding author:
e-mail: 100057569@ku.ac.ae

Abstract Increased population and urbanization have resulted in the generation of significant amounts of wastewater. The integration of membrane technology with nanotechnology has prompted revolutionary advances in the treatment of wastewaters. In this study, functionalized multi-walled carbon nanotubes (f-MWCNT)- (GO) nanocomposite was prepared by self-assembly, then incorporated into polylactic acid (PLA) membranes. Different concentrations of f-MWCNT-GO ranging from 0% to 8 wt.% were used. Fourier-transform infrared (FTIR) was performed to confirm the existence of f-MWCNT-GO in the fabricated membranes. In addition, the effect of f-MWCNT-GO incorporation on the performance of the membranes were investigated by carrying out analyses that include, but are not limited to, deionized (DI) water contact angle (CA), porosity, water flux, heavy metals removal, etc. The addition of f-MWCNT-GO resulted in a decrease in the DI water CA from 79.0±3.8° in the pristine PLA membrane to 51.8±2.4° in the 8 wt.% f-MWCNT-GO-PLA membrane. Furthermore, the water flux increased from 1062.8 L/m^2·h to 2543.4 L/m^2·h in the pristine PLA and 8 wt.% f-MWCNT-GO-PLA membrane, respectively. Such membranes have the potential to be utilized in real wastewater treatment applications.

Keywords: Wastewater; functionalized multi-walled carbon nanotubes; graphene oxide; Self-assembly; nanocomposite.

1. Introduction

In recent years, increased attention have been given to the recycling of wastewater as an alternative that can help in to reducing the growing water scarcity in many regions (Van Loosdrecht & Brdjanovic, 2014). Membrane processes such as ultrafiltration (UF) has attracted significant attention in the management of wastewater due to its easier application, higher removal efficiency, lower energy consumption, and reduced environmental footprint (Purkait & Singh, 2018). The properties of these membranes can be further improved through the incorporation of nanomaterial into the matrix of the membrane. These nanomaterials include carbon nanotubes (CNTs), zeolites, zirconium phosphate, metal oxides, graphene oxide (GO), aluminum oxide (Al_2O_3), among many others (Daer et al., 2015) (Goh et al., 2015). Furthermore, different polymers are currently utilized to fabricate membranes which include, but are not limited to, polyether sulfone (PES), polypropylene (PP), polytetrafluoroethylene (PTFE), polyvinylidene fluoride (PVDF), polyamide, cellulose acetate (CAs), among others. These fossil-based polymers can have negative impacts on the environment both upon disposable or during the manufacturing process(Zhou et al., 2011). Furthermore, the growing environmental pollution of plastics wastes has been the starting point for researching potential natural polymers able to substitute the traditional ones for membrane preparation. One of the attractive examples of the natural polymers being used currently for the preparation of membranes is polylactic acid (PLA). The PLA polymer has low toxicity, decent biodegradability, biocompatibility, and can be recycled easily(Galiano et al., 2018). Hence, the usage of PLA is believed to serve as an efficient and environmentally friendly solution with a reduced carbon footprint. Nevertheless, pristine PLA membranes have lower rejection of contaminates. Therefore, in this study, f-MWCNT-GO nanocomposite was prepared and used as a filler in the PLA membrane matrix to enhance their overall properties. The f-MWCNT-GO-PLA membranes were fabricated via phase inversion method and then their performance was evaluated through different water filtrations tests, heavy metal ions removal, among others. In addition, the membranes were characterized using different techniques that include DI water contact angle (CA), FT-IR, porosity, mean pore size, among others.

2. Experimental

2.1 Materials

PLA pellets were obtained from Good Fellow Co., UK. N, N-Dimethylacetamide (DMAc) (Mw = 87.12 g/mol, purity of ≥99%), polyvinylpyrrolidone (PVP, Mw: 40 kDa), copper nitrate ($Cu(NO_3)_2$), nickel chloride ($NiCl_2$) and zinc chloride ($ZnCl_2$) were all purchased from Sigma-Aldrich. HACH detection cuvettes were used to measure the concentration of heavy metals in wastewater and treated filtrate using HACH DR3900 UV/Vis spectrophotometer.

2.2 Synthesis of the nanocomposite

Pure MWCNTs was added to a prepared acid mixture of H_2SO_4/HNO_3 (3:1 by volume ratio). EDC, NHS and ethylenediamine (ED) were added to the mixture for the functionalization step. GO was prepared following themodified Hummers' method (Huang et al., 2011). f-MWCT and GO were self-assembled at a ratio of 60:40, respectively.

2.3 Membrane fabrication

Five membranes were fabricated, as shown in Table 1.

Table 1. Membrane's composition

Mem. ID	PLA (%)	DMAC (%)	nanocomposite (wt.%)*	PVP (%)
P	15	83	0	2
M2	15	83	2	2
M4	15	83	4	2
M6	15	83	6	2
M8	15	83	8	2

*With respect to the PLA polymer

The nanocomposite was sonicated in DMAC for 1 h, then PLA and PVP were slowly added to the solution and kept stirring for 24 h. The solution was then put in vacuum oven for degassing purposes for 1 h and on the shelf for another hour prior to casting it on a non-woven support fixed on a glass plate using a 200 μm membrane casting knife. Following that, the membranes were immediately submerged in DI water coagulation bath.

2.4 Characterization of pristine and PLA/f-MWCNT-GO membranes

A static CA value was obtained for each membrane using the Krüss GmbH' Drop Shape Analyzer (DSA). The functional groups of the prepared membranes were analyzed via FT-IR spectroscopy using Bruker Vertex 80v spectrometer. All samples were scanned for 64 times with a resolution of 4 cm^{-1} and a wavelength range between 400–2000 cm^{-1}. The porosity of the membranes was determined using the dry-wet method. Initially, membrane samples were dried in a vacuum oven at 60 °C for 2 h, and their weight was recorded (W_d). Then, the samples were soaked in DI water for 24 h under stirring and their weight was measured after removing all excess liquid (W_w). The porosity ε (%) was calculated using Eq. (1):

$$\varepsilon\ (\%) = ((Ww - Wd)/(\rho w * \delta * A))*100 \quad (1)$$

Where A is the effective area of the membrane, ρw is the density of DI water, and δ is the membrane total thickness.

2.5 Preparation of synthetic metal mixture wastewater solution and heavy metals rejection

Synthetic metal mixture wastewater solution was prepared by dissolving copper nitrate, nickel chloride and zinc chloride in 3 L of DI water. The final synthetic wastewater contained 8 , 5 and 6 mg/L concentrations of Cu (II), Ni (II) and Zn (II), respectively. LCK HACH vials using HACH DR3900 UV/Vis spectrophotometer was used to calculate the concentration of heavy metals before (Cf) and after (Cp) filtration. The removal efficiency (%) of heavy metals was calculated using the following Eq. (2):

$$R(\%) = (1- Cf/ Cp)*100 \quad (2)$$

2.6 Performance of pristine and PLA/f-MWCNT-GO membranes

A stirred dead-end ultrafiltration cell, along with a compressed air cylinder were utilized to obtain pure water flux measurements. A pressure of 30 psi was first applied for 30 mins for compaction purposes. This step is important to prevent pores collapse and to stabilized the performance of the membranes. The pressure was then reduced to 20 psi to and the water flux measurements were recorded for 1 h. DI water was used for the pure water flux ($L/m^2 \cdot h$) and was calculated using Eq. (3):

$$Flux(\ L/m^2 \cdot h) = V/A*t \quad (3)$$

Where V is the collected water volume, and t is the time needed to collect the water.

3. Results and discussion

3.1 FT-IR analysis

FTIR spectra of the pristine PLA and composite membranes are shown in Fig. 1. The stretching vibrations at 1020 cm^{-1} (C–OH and C–O–C merged) and 1401 cm^{-1} (C–OH stretching) are due to the presence of GO (Vijay Kumar et al., 2013). Since the MWCNTs are functionalized, the existence of the amine groups is shown by the peaks at 1489 cm^{-1} (C–N) and 1051 cm^{-1} (N–H). Characteristic absorption bands at 1100 cm^{-1} and 1710 cm^{-1} correspond to the stretching vibrations of -C-O and -C=O ester groups of PLA (Y. Zhou et al., 2018). It is noticeable that the characteristic peaks of PLA were still dominant upon the addition of the nanocomposite and no new peaks were formed with the increase in the nanocomposite content. In other words, the addition of the nanocomposite did not affect the structure of PLA. However, with the increase of the nanocomposite content, the PLA peaks became less sharp and shifted slightly higher. Along with the existence of GO and f-MWCNTs peaks in the spectra, all this does prove that the nanocomposite was successfully embedded into the polymer matrix.

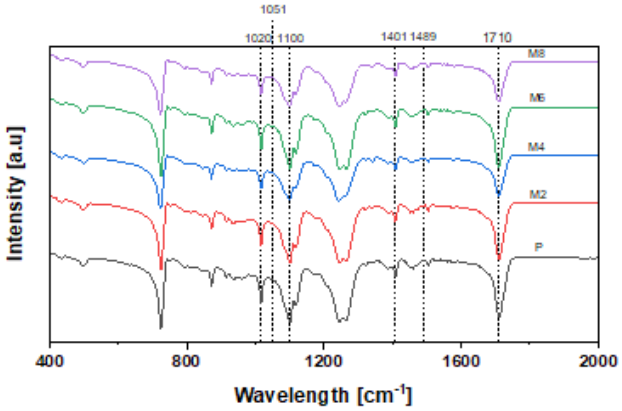

Figure 1. FTIR spectrum of the pristine PLA and composite membranes

3.2 Contact angle, porosity and flux analyses

The porosity measurements of the pristine PLA and composite membranes are summarized in Figure 2. As can be observed from the figure, the porosity of the composite membranes improved significantly. For example, the porosity increased from 27% in the pristine PLA membrane to as high as 41% in the M8 membrane (8 wt.% f-MWCNT-GO nanocomposite). Similarly, the DI water CA decreased (i.e., hydrophilicity enhancement) after the addition of the nanocomposite. For instance, the DI CA of the pristine PLA membrane was around 79º and this dropped to as low as 52º in the M8 membrane. The improvements in the hydrophilicity and porosity of the composite membranes can be directly linked to the hydrophilic nature of the nanocomposite used. During the phase inversion step, the hydrophilic nanocomposite attracts more water molecules which creates more water penetration sites on the surface of the membrane. This eventually causes the surface of the membrane to become more porous (Ibrahim et al., 2020). These improved properties have direct impact on the DI water flux of the membranes. As illustrated in Figure 4, the DI water flux of the composite membranes increased significantly. The highest water flux was observed in the M8 membrane with around 2543 L/m^2·h. This is 2.5 times higher than the pristine PLA membrane which reported DI water flux of only 1062 L/m^2·h (Figure 4).

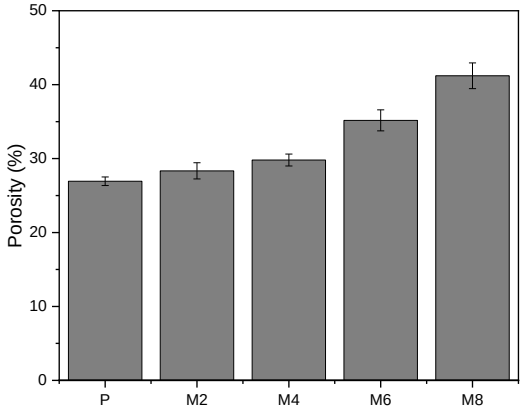

Figure 2. Membrane porosity of the pristine PLA and composite membranes

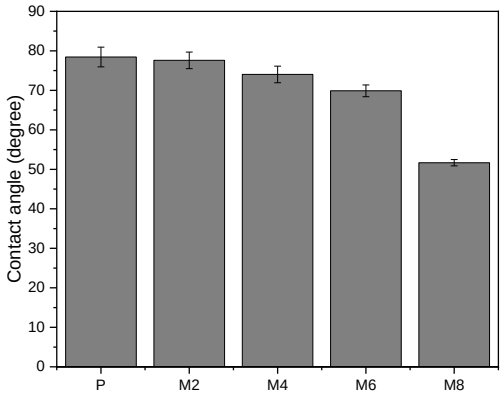

Figure 3. Contact angle of the pristine PLA and composite membranes

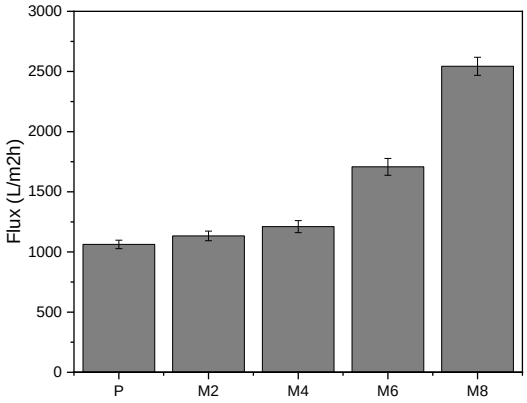

Figure 4. Water flux of the pristine PLA membrane and composite membranes

3.3 Heavy metals rejection

The performance of the pristine PLA and composite membranes in terms of heavy metal ions rejection is summarized in Figure 5. The composite membranes showed slight improvement in the heavy metal ions rejection at pH=7. For instance, the Cu2+ removal increased from 81% to 85% in the pristine PLA and M8 membranes, respectively. Similar observations can be seen in the case of Ni2+ removal. These slight improvements in the heavy metal ions rejection can be related to the improved surface charge of the composite membranes (i.e., presence of different functional groups). This will improve the electrostatic attraction between the positively charged metal ions and the negatively charged membrane surface. Furthermore, at pH=7, metal ions can form complexes with the different functional groups present at the surface of the membrane as well as other coexisting anions (Cl^{-1}, NO_3^{-1}, OH^{-1}) and thereby increases the size of the metal ions. Also, the metal ions have the potential of forming metal hdyroxides which have increased overall size. These occurances lead to eventual exclusion of the heavy metal ions via size exclusion.

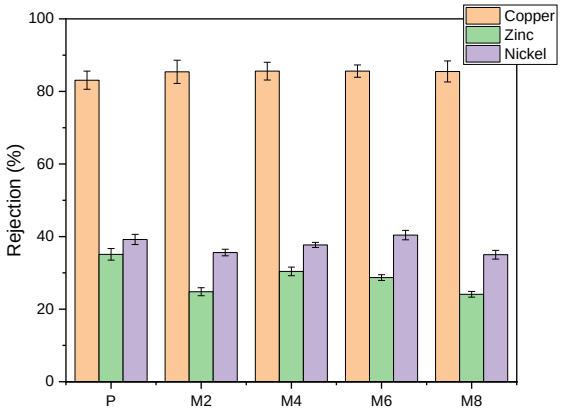

Figure 5. Heavy metals rejection using the pristine PLA and composite membranes

4. Conclusion

In this study, PLA/f-MWCNT-GO membranes were fabricated via phase inversion method and were tested for their potential application in wastewater treatment. The membranes showed slight improvement in the heavy metal ions rejection. On the other hand, substantial increased in the DI water flux was observed. The water flux increased from 1062.8 L/m^2·h to 2543.4 L/m^2·h in the pristine PLA and 8 wt.% f-MWCNT-GO-PLA membrane, respectively These results concluded that the addition of the nanocomposite (f-MWCNT-GO) has improved the properties of the membrane. Such improvements can open doors for the application of these composite membranes in real wastewater treatment.

References

Daer, S., Kharraz, J., Giwa, A., & Hasan, S. W. (2015). Recent applications of nanomaterials in water desalination: A critical review and future opportunities. In *Desalination* (Vol. 367, pp. 37–48). Elsevier. https://doi.org/10.1016/j.desal.2015.03.030

FTIR spectrum of PLA. Depicted are the characteristic absorption bands... | Download Scientific Diagram. (n.d.). Retrieved April 20, 2021, from https://www.researchgate.net/figure/FTIR-spectrum-of-PLA-Depicted-are-the-characteristic-absorption-bands-at-1-740-1-183_fig2_323818622

Galiano, F., Briceño, K., Marino, T., Molino, A., Christensen, K. V., & Figoli, A. (2018). Advances in biopolymer-based membrane preparation and applications. In *Journal of Membrane Science* (Vol. 564, pp. 562–586). Elsevier B.V. https://doi.org/10.1016/j.memsci.2018.07.059

Goh, P. S., Ng, B. C., Lau, W. J., & Ismail, A. F. (2015). Inorganic nanomaterials in polymeric ultrafiltration membranes for water treatment. *Separation and Purification Reviews*, *44*(3), 216–249. https://doi.org/10.1080/15422119.2014.926274

Huang, N. M., Lim, H. N., Chia, C. H., Yarmo, M. A., & Muhamad, M. R. (2011). Simple room-temperature preparation of high-yield large-area graphene oxide. *International Journal of Nanomedicine*, *6*, 3443–3448. https://doi.org/10.2147/ijn.s26812

Ibrahim, Y., Naddeo, V., Banat, F., & Hasan, S. W. (2020). Preparation of novel polyvinylidene fluoride (PVDF)-Tin(IV) oxide (SnO2) ion exchange mixed matrix membranes for the removal of heavy metals from aqueous solutions. *Separation and Purification Technology*, *250*, 117250. https://doi.org/10.1016/j.seppur.2020.117250

Purkait, M. K., & Singh, R. (2018). Membrane Technology in Separation Science. In *Membrane Technology in Separation Science*. CRC Press. https://doi.org/10.1201/9781315229263

Van Loosdrecht, M. C. M., & Brdjanovic, D. (2014). Anticipating the next century of wastewater treatment. In *Science* (Vol. 344, Issue 6191, pp. 1452–1453). American Association for the Advancement of Science. https://doi.org/10.1126/science.1255183

Vijay Kumar, S., Huang, N. M., Lim, H. N., Marlinda, A. R., Harrison, I., & Chia, C. H. (2013). One-step size-controlled synthesis of functional graphene oxide/silver nanocomposites at room temperature. *Chemical Engineering Journal*, *219*, 217–224. https://doi.org/10.1016/j.cej.2012.09.063

Zhou, J., Chang, V. W. C., & Fane, A. G. (2011). Environmental life cycle assessment of reverse osmosis desalination: The influence of different life cycle impact assessment methods on the characterization results. *Desalination*, *283*, 227–236. https://doi.org/10.1016/j.desal.2011.04.066